ELSEVIER

Journal of Power Sources 81–82 (1999) 306–311

JOURNAL OF POWER SOURCES

www.elsevier.com/locate/jpowsour

XPS analysis of the lithium intercalation in amorphous tungsten oxysulfide thin films

I. Martin [a,*], P. Vinatier [a], A. Levasseur [a], J.C. Dupin [b], D. Gonbeau [b]

[a] *Institut de Chimie de la Matière Condensée de Bordeaux, CNRS, and Ecole Nationale Supérieure de Chimie et Physique de Bordeaux, Avenue Pey Berland, BP 108, 33402 Talence Cedex, France*

[b] *Laboratoire de Physico - Chimie Moléculaire (UMR 5624), Université de Pau et des Pays de l'Adour, 2, Avenue du Président Angot, 64000 Pau, France*

Abstract

Amorphous thin films of tungsten oxysulfide have been prepared by radio frequency (RF) magnetron sputtering. The composition of thin films is varied by changing the pressure of the reactive gas (O_2) and discharge gas ($Ar + O_2$) in the sputtering chamber. The X-ray photoelectron spectroscopy (XPS) studies of the thin films have shown three different types of environment for tungsten atoms: W^{6+} surrounded by oxygen O^{2-}, W^{4+} surrounded by sulphur S^{2-} and W^{5+} in a mixed oxygen–sulphur environment consisting of O^{2-}, S^{2-} and S_2^{2-} pairs. The electrochemical characterisation of the film was performed in the $Li/LiPF_6$-EC-DMC/WO_yS_z cell. The XPS during intercalation evidences the role of W^{6+} and S_2^{2-} in the redox process. © 1999 Elsevier Science S.A. All rights reserved.

Keywords: Thin films; XPS analysis; Lithium batteries; RF magnetron sputtering; Transition element oxysulfide

1. Introduction

After several studies on titanium oxysulfide which are used as thin film positive electrode in prototype of micro-batteries [1–3], molybdenum and tungsten oxysulfide were investigated in order to involve more oxidation states of the transition element in redox mechanisms occurring during intercalation and de-intercalation of lithium in these materials [4–8]. The present work reports the initial results obtained with tungsten.

2. Experimental

Tungsten oxysulfide thin films have been deposited using radio frequency (RF) magnetron sputtering at room temperature. Polycrystalline 2H–WS_2 (where the tungsten is in a trigonal prismatic environment) was used as target. The sputtering was carried out with a target–substrate distance of 7 cm. The chamber was evacuated to less than 10^{-4} Pa before introducing argon as discharge gas. Oxygen reactive gas can be introduced in the chamber to increase oxygen content in the thin films; its pressure was chosen between 2.10^{-4} to 10^{-2} Pa. The discharge gas was then introduced, and the final pressure being between 1 to 5 Pa.

Thin films were deposited with different oxygen and total pressure values, within the range mentioned above to obtain different composition thin films.

The chemical composition of thin films was determined by Rutherford backscattering spectroscopy (RBS). Thin films were characterised by X-ray diffraction using a PW 1730 Philips diffractometer with the CuKα radiation. The thickness, texture and surface morphology of the films were analysed by scanning electron microscope (Jeol JSM-5200). Electronic conductivity of the thin films deposited on an insulating glass substrate was measured by four-probe method.

The X-ray photoelectron spectroscopy (XPS) analyses were performed with a Surface Science Instruments spectrometer (Model 301) using a focused monochromatized AlKα radiation (1486.6 eV). The diameter of the irradiated area was 300 μm, and the residual pressure inside the analysis chamber was in the 5.10^{-8} Pa range. The spectrometer was calibrated by using the photoemission lines of Au ($Au_{4f7/2} = 83.9$ eV, with reference to the Fermi

* Corresponding author

0378-7753/99/$ - see front matter © 1999 Elsevier Science S.A. All rights reserved.
PII: S0378-7753(99)00129-9

level) and Cu ($Cu_{2p3/2}$ = 932.5 eV); for the $Au_{4f7/2}$ line, the full width at half maximum (FWHM) was 0.86 eV in the recording conditions (the peaks were recorded with a constant pass energy of 50 eV). For the WO_yS_z and $Li_xWO_yS_z$ thin films, the XPS analyses presented were done after mechanical erosion under high vacuum. For the tungsten oxides, the calibration of binding energy scale was done with the C_{1s} line (284.6 eV) from the carbon contamination layer. The XPS signals were analysed using a peak synthesis program in which a non-linear background is assumed and the fitting peaks of the experimental curve are defined using combination of Gaussian (80%) and Lorentzian (20%) distribution.

The electrochemical characterisation of the film was performed in the $Li/LiPF_6$-EC-DMC/WO_yS_z cell. The batteries were intercalated and deintercalated galvanostatically with a current of 1 μA. The XPS measurements of thin films were carried out at different stages of the discharge.

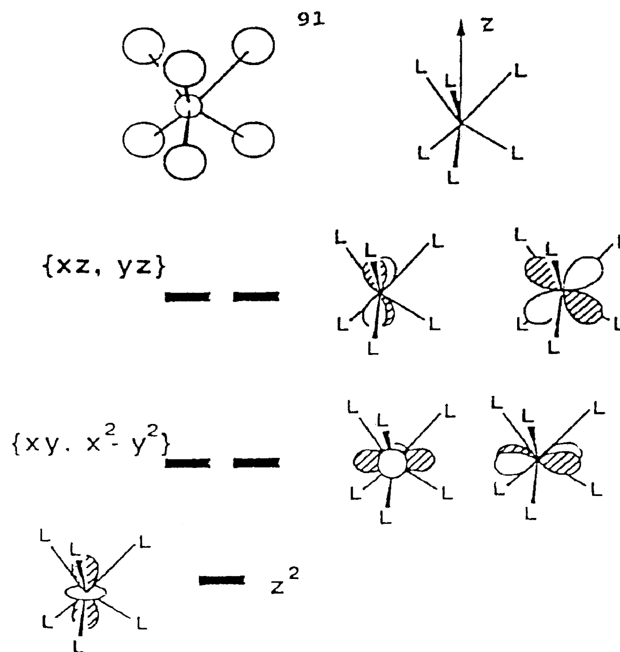

Fig. 1. Energy level in a trigonal prismatic environment of WS_2.

3. Results and discussion

The composition of thin films depends on the sputtering condition, mainly the pressure of the gases. In Table 1, the composition of thin films obtained by RBS studies and the corresponding sputtering conditions are shown. A wide range of composition can be obtained using RF magnetron sputtering. When the oxygen pressure increases, keeping the total pressure constant, the oxygen content y increases. Similar increase in y is observed when the total pressure increases for a constant oxygen pressure in the plasma. The amorphous nature of the thin films was evidenced by the X-ray analysis. The scanning electron microscopy (SEM) studies have shown that after 4 h of sputtering, the thin films were about 1 μm in thickness and the growth is perpendicular to the substrate.

The electronic conductivity measurements were carried out on thin films with composition $WO_{0.6}S_{1.7}$, $WO_{0.8}S_{1.6}$ and $WO_{2.9}S_{0.5}$ and on the polycrystalline 2H–WS_2. According to the energy level of WS_2 (W in a trigonal prismatic environment; Fig. 1) [9–11], 2H–WS_2 is semiconducting and the gap between the full d_{z^2} and the $d_{x^2-y^2}$ and d_{xy} half full is about 1.3 eV. The temperature dependence of electronic conductivity ($\log\sigma$ vs. 1000/T plots) for different composition of thin films are shown in Fig. 2. It can be seen that the films are semiconducting. For $WO_{0.6}S_{1.7}$ and $WO_{0.8}S_{1.6}$, XPS analysis shows that the W^{4+} (d^2) are predominant. The d_{z^2} are full and the electronic transition is possible. The conductivity at 300 K is of the order of 0.06 Ω^{-1} cm^{-1} and 0.022 Ω^{-1} cm^{-1}, respectively. For $WO_{2.9}S_{0.5}$, the behaviour is semiconducting too, but the conductivity is very low, 0.75×10^{-7} Ω^{-1} cm^{-1}; in this case, XPS shows that W^{6+} (d^0) is mainly present, the d_{z^2} band is empty so the electronic transition is very difficult.

Table 1
Composition of WO_yS_z thin films determined by Rutherford backscattering spectroscopy (RBS)

Po_2 (Pa)	P_{total} (Pa)	Composition WO_yS_z
0	1	$WO_{0.6}S_{1.7}$
10^{-3}	1	$WO_{0.9}S_{1.9}$
10^{-3}	5	$WO_{1.1}S_{1.7}$
4.10^{-3}	5	$WO_{3.0}S_{0.3}$

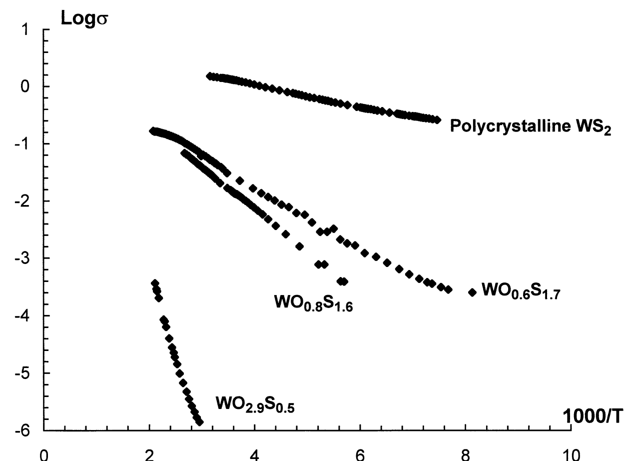

Fig. 2. Electronic conductivity of three thin films with composition $WO_{0.6}S_{1.7}$, $WO_{0.8}S_{1.6}$ and $WO_{2.9}S_{0.5}$ and of polycrystalline WS_2.

4. XPS analysis

A preliminary step before the analysis of XPS spectra was the characterisation of some reference compounds: WO_2, WO_3, WS_2 and WS_3. Then chemical species and the different tungsten environments in thin films were examined. For easier presentation, our discussion deals with formal oxidation numbers associated with full charges although in reality, many gradations can exist.

4.1. Reference compounds

Three significant environments for the transition metal were associated with the following formal oxidation numbers: +4 for WO_2 and WS_2, +6 for WO_3. In order to characterise disulphide pairs, the analysis of WS_3 was carried out. The values for WS_2, WO_3 and WO_2 correspond to those generally reported. For WS_3, S_{2p} XPS peak shows two partially overlapping doublets attributed to S_2^{2-} pairs (on the high energy side) and to S^{2-} sulphur (on the low energy side) in a 1:2 proportion as observed in the previous work of Khudorozhko et al. [12]. The whole W_{4f} and S_{2p} peaks are listed in Table 2.

4.2. $WO_{2.9}S_{0.5}$ thin film

The $WO_{2.9}S_{0.5}$ composition thin film has been studied. In view of the previous results, W_{4f} peak was divided into three components (Fig. 3). Besides the full oxidised W^{6+} as in WO_3 corresponding to the peak C (35.8–38.0 eV) and the W^{4+} similar to those in WS_2 matching to peak A (32.8–35.0 eV), an intermediate B doublet is observed. Early studies show that its relative intensity, in comparison with peak A, enhances with the progressive amount of oxygen in the thin films. Considering this evolution and the associated binding energy (34.2–36.4 eV) at a higher value than that of the sulphur environment, the binding energy of B being close to values reported in the case of H_xWO_3 bronzes [13] and for WO_{3-x} [14], +5 formal oxidation state was associated to this peak.

With XPS being not quantitative, it is impossible to have a precise view of the amount of each ions. At room temperature, thin films are homogeneous, it is not a mixture of WO_3, WS_2 and WO_yS_z.

A previous study on molybdenum oxysulfides have shown the same type of behaviour. In addition, after annealing of these thin films, a mixture of MoO_2 and MoS_2 appears clearly.

For the tungsten oxysulfides the same study is in progress.

The variation of the intensity of the three peaks of sulphur with the composition of different thin films allowed to assign the oxidation states of sulphur (Fig. 4). It was shown that when the oxygen content increases, both peak F (disulphides pairs) (163.2–164.3 eV) and peak D (161.5–162.6 eV) increase, while peak E (S^{2-} sulphur) (162.2–163.4 eV) clearly decreases. In these conditions, these two kinds of sulphur ions could be associated with the mixed oxygen–sulphur environment of tungsten characterised by the peak B. This observation may imply a new environment for tungsten atoms surrounded by O^{2-} ions, S_2^{2-} ions and S^{2-} ions (different from those present in WS_2); this last type will be indicated as S^{2-}(me) as mixed environment in the following.

In the amorphous thin films, the tungsten ions have three different environments with three different oxidation states:

(i) W^{4+} (peak A) in a sulphur environment [S^{2-} (peak E)];

(ii) W^{5+} in a mixed oxygen–sulphur environment [O^{2-}, S_2^{2-} pairs (peak F) and S^{2-} (peak D) more negative than S^{2-} (peak E)]; and

(iii) W^{6+} (peak C) in an oxygen environment (O^{2-}).

4.3. Lithium intercalation

The analysis of lithium intercalation was studied for a thin film $WO_{2.9}S_{0.5}$ composition. Figs. 3 and 4 report the W_{4f} and S_{2p} peaks before intercalation (OCV = 3.1 V) and at two stages of the first discharge (intercalation of lithium OCV = 2.17 V and 1.8 V).

During the intercalation (OCV = 2.17 V), very significant changes in the W_{4f} and S_{2p} peaks are observed. The C doublet (W^{6+} as in WO_3) clearly decreases and the A and B doublets simultaneously increase (Fig. 3). A general peak widening can be noted, which should indicate some structural perturbances involved by the lithium insertion. These results show clearly a W^{6+} reduction.

Concerning the S_{2p} peak during intercalation of lithium (Fig. 4), an increase of the E doublet (S^{2-} sulphur as in WS_2) and of the D peak [S^{2-}(me)] was observed while on

Table 2
W_{4f} and S_{2p} binding energies (eV) in the reference compounds [relative atomic percentage in hooks]

	$W_{4f\,7/2-5/2}$	$S_{2p\,3/2-1/2}$
WO_3	35.6–37.8 (1.2)(1.2)	
WO_2	32.9–35.1 (1.7)(1.7)	
WS_2 polycrystalline	32.8–35.0 (1.0)(1.0)	162.4–163.6 (0.9)(0.9)
WS_2 single crystal	33.0–35.2 (0.85)(0.9)	162.6–163.8 (0.9)(0.9)
WS_3	33.0–35.2	162.3–163.4 [67%] (1.2)(1.2)
		163.5–164.6 [33%] (1.2)(1.2)

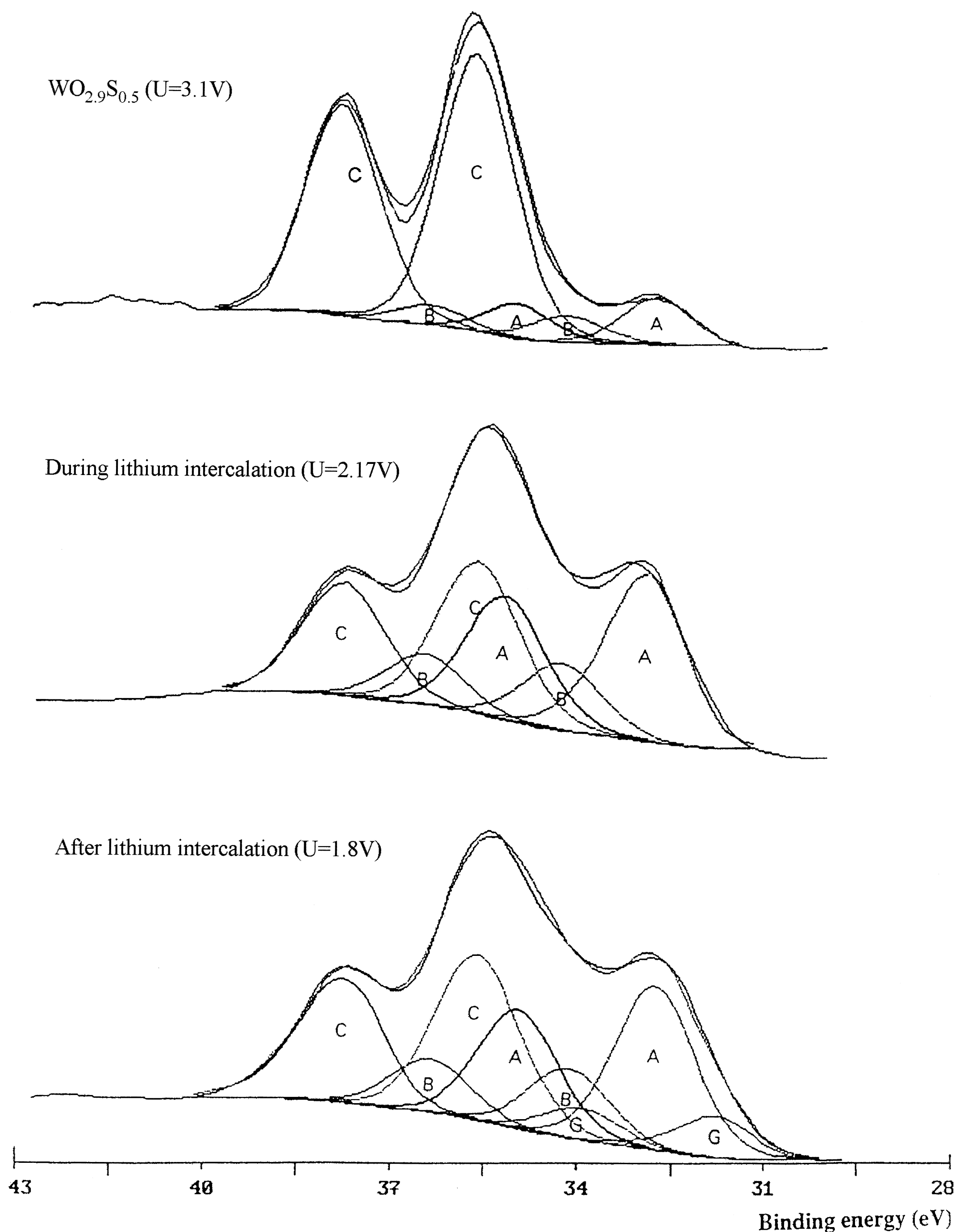

Fig. 3. $WO_{2.9}S_{0.5}$: evolution of the W_{4f} peak during lithium intercalation and after lithium intercalation.

the high energy side, the F doublet (S_2^{2-} sulphur pairs) strongly decreases. The disulphide groups are also involved in the redox process.

At the 1.8 OCV potential, no decisive variation occurs in the high energy side but an evolution of the signal shape undergoes for the low energy side. This corresponds to a slight decrease of the component A and simultaneously, a new component (G) appears the low energy side; its binding energy (31.8–34.0 eV) is close to the value of the tungsten W^0 doublet (31.6–33.8 eV—W metal). Obviously, it is not a metallic cluster but only after reduction, the d-level of the W atoms are full. That kind of oxidation state has already been observed for MoS_3 [15] and for MoO_yS_z thin films [8]. The phenomenon is also very similar than the one observed by Brec [16]. He has shown that in $NiPS_3$, Ni^0 is present after intercalation.

In the case of S_{2p} peak after intercalation, F doublet keeps decreasing in the same way as E doublet. In parallel,

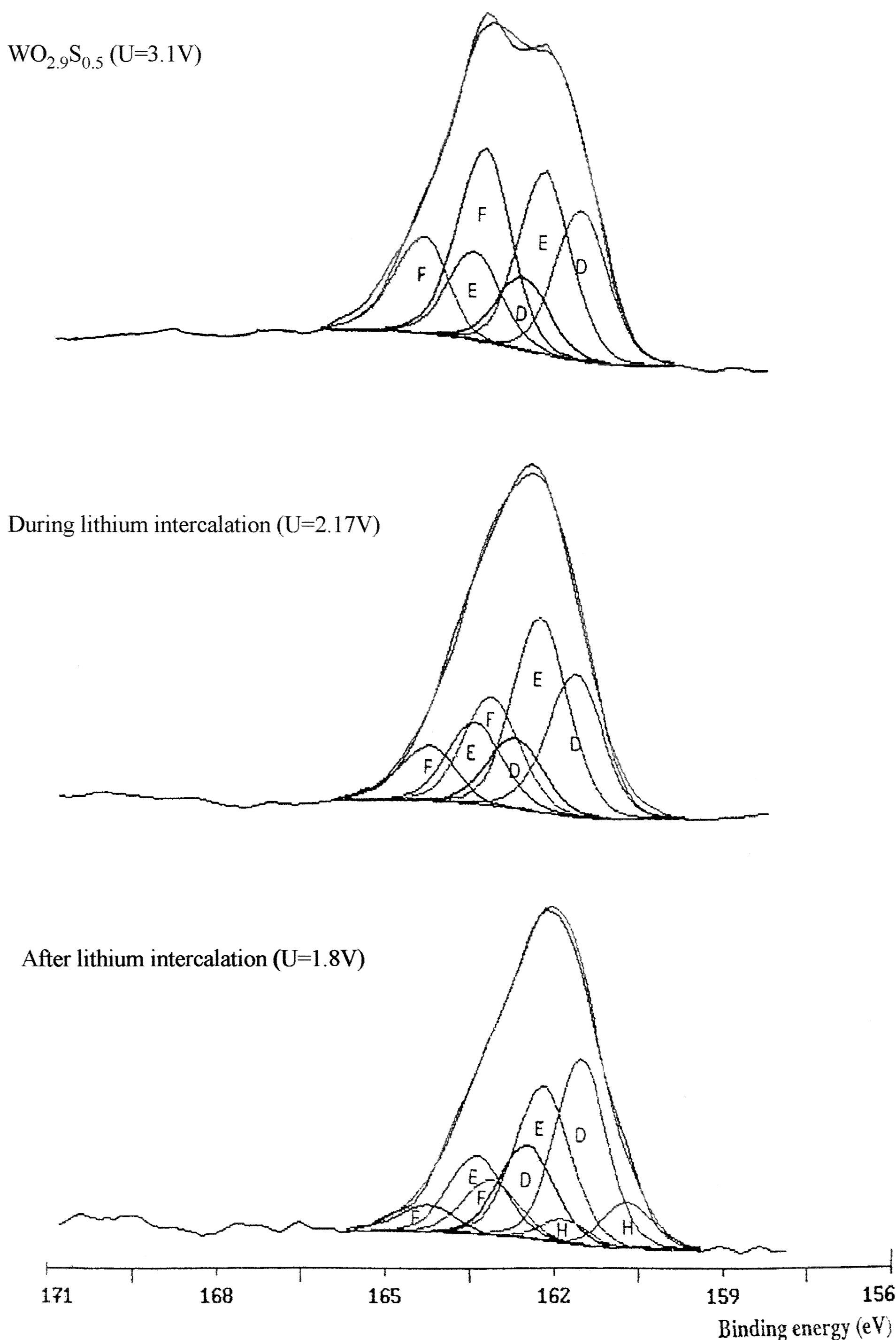

Fig. 4. $WO_{2.9}S_{0.5}$: evolution of the S_{2p} peak during lithium intercalation and after lithium intercalation.

an increase of the component D is observed. In addition, a new component (H) is introduced in order to fit the final shape on the low energy side; its binding energy (160.8–161.9 eV) is similar to the value obtained for S^{2-} sulphur in Li_2S (160.7–161.9 eV). These results show a reduction of S_2^{2-} sulphur pairs and S^{2-} ions (as in WS_2) in sulphur atoms characterised by a more negative real charge S^{2-}(me) and S^{2-} as found in Li_2S.

Through XPS results obtained with the intercalation of lithium in an oxygen-rich film, it has appeared that S_2^{2-} sulphur pairs and W^{6+} ions are the main species involved in the redox process. First, a reduction of W^{6+} to W^{5+} and to W^{4+} occurs, then the redox process continues with formation of W^0. Simultaneously, the S_2^{2-} sulphur pairs are reduced to two different types of S^{2-} ions S^{2-}(me) and S^{2-} (as in Li_2S).

5. Conclusions

The results have clearly demonstrated the specific character of WO_yS_z thin films with the existence of several environments for both tungsten atoms (W^{6+}, W^{5+} and W^{4+}) and sulphurs ones [S_2^{2-}, S^{2-} (WS_2) and S^{2-} (more negative than the previous one)].

The XPS analysis had permitted to put in evidence an important contribution of the sulphurs as well as the transition metal during the redox mechanisms of discharge. Several other compositions specifically with lower oxygen content are studied in order to increase the current density allowable in such kind of materials and to confirm these first results.

References

[1] G. Meunier, R. Dormoy, A. Levasseur, Mater. Sci. Eng. B 3 (1989) 19.
[2] D. Gonbeau, C. Guimon, G. Pfister-Guillouzo, A. Levasseur, G. Meunier, R. Dormoy, Surf. Sci. 254 (1991) 81.
[3] G. Meunier, R. Dormoy, A. Levasseur, Thin Solid Films 205 (1991) 213.
[4] E. Schmidt, F. Weill, G. Meunier, A. Levasseur, Thin Solid Films 245 (1994) 34.
[5] L. Benoit, D. Gonbeau, G. Pfister-Guillouzo, E. Schmidt, G. Meunier, A. Levasseur, Surf. Interface Anal. 22 (1994) 206.
[6] E. Schmidt, G. Meunier, A. Levasseur, Solid State Ionics 76 (1995) 243.
[7] L. Benoit, D. Gonbeau, G. Pfister-Guillouzo, E. Schmidt, G. Meunier, A. Levasseur, Thin Solid Films 258 (1995) 110.
[8] L. Benoit, D. Gonbeau, G. Pfister-Guillouzo, E. Schmidt, G. Meunier, A. Levasseur, Solid State Ionics 76 (1995) 81.
[9] K.A. Yee, T. Hughbanks, Inorg. Chem. 30 (1991) 2321.
[10] J.A. Wilson, A.D. Yoffe, Adv. Phys. 18 (1969) 193.
[11] P.M. Williams, F.R. Shepherd, J. Phys. C 6 (1973) L36.
[12] G.F. Khudorozhko, I.P. Asanov, L.N. Mazalov, E.A. Kravtsova, G.K. Parygina, V.E. Fedorov, Ju.V. Mironov, J. Electron. Spectrosc. Rel. Phen. 68 (1994) 199.
[13] G. Hollinger, Vide, Couches Minces 201 (1980) 405.
[14] R. Gehlig, E. Salje, A.F. Carley, M.W. Roberts, J. Solid State Chem. 49 (1983) 318.
[15] R.A. Scott, A.J. Jacobson, R.R. Chianelli, W.H. Pan, E.I. Stiefel, K.O. Hodgson, S.P. Cramer, Inorg. Chem 25 (1986) 1461.
[16] R. Brec, Solid State Ionics 22 (1986) 3–30.